Communication

Molecular Modeling Based Approach to Potent P2–P4 Macrocyclic Inhibitors of Hepatitis C NS3/4A Protease

Nigel J. Liverton, M. Katharine Holloway, John A. McCauley, Michael T. Rudd, John W. Butcher, Steven S. Carroll, Jillian DiMuzio, Christine Fandozzi, Kevin F. Gilbert, Shi-Shan Mao, Charles J. McIntyre, Kevin T. Nguyen, Joseph J. Romano, Mark Stahlhut, Bang-Lin Wan, David B. Olsen, and Joseph P. Vacca

J. Am. Chem. Soc., **2008**, 130 (14), 4607-4609 • DOI: 10.1021/ja711120r

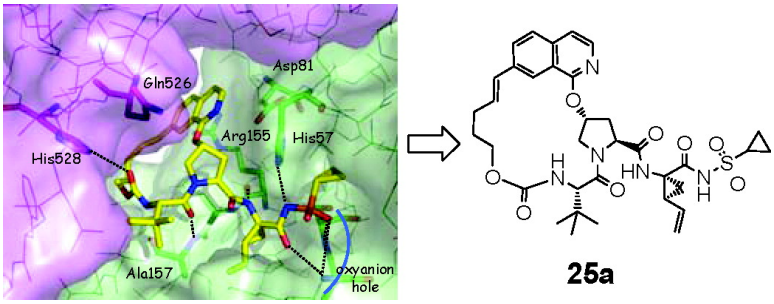

More About This Article

Additional resources and features associated with this article are available within the HTML version:

- Supporting Information
- Links to the 4 articles that cite this article, as of the time of this article download
- Access to high resolution figures
- Links to articles and content related to this article
- Copyright permission to reproduce figures and/or text from this article

View the Full Text HTML

J|A|C|S
COMMUNICATIONS

Published on Web 03/14/2008

Molecular Modeling Based Approach to Potent P2−P4 Macrocyclic Inhibitors of Hepatitis C NS3/4A Protease

Nigel J. Liverton,*,‡ M. Katharine Holloway,§ John A. McCauley,‡ Michael T. Rudd,‡ John W. Butcher,‡ Steven S. Carroll,† Jillian DiMuzio,† Christine Fandozzi,|| Kevin F. Gilbert,‡ Shi-Shan Mao,† Charles J. McIntyre,‡ Kevin T. Nguyen,‡ Joseph J. Romano,‡ Mark Stahlhut,† Bang-Lin Wan,|| David B. Olsen,† and Joseph P. Vacca‡

Departments of Medicinal Chemistry, Antiviral Research, Drug Metabolism, and Molecular Systems, Merck Research Laboratories, West Point, Pennsylvania 19486

Received December 19, 2007; E-mail: nigel_liverton@merck.com

Worldwide, 170−200 million people are chronically infected with the hepatitis C virus (HCV).[1] The positive RNA strand *Flaviviridae* virus replicates primarily in the liver, and while disease progression is typically a slow process occurring over many years, ultimately a significant fraction develops serious liver disease including cirrhosis and hepatocellular carcinoma.[2] HCV is currently a leading cause of death in HIV coinfected patients[3] and is the most common basis for liver transplantation surgery.[4] Several promising antiviral targets for HCV have emerged in recent years,[5] with NS3/4A protease inhibitors showing perhaps the most dramatic antiviral effects.[6] Clinical proof of concept has been demonstrated both for rapidly reversible inhibitors and slowly reversible ketoamide active site serine trap compounds such as BILN-2061 (**1**)[7] and VX-950 (telaprevir, **2**),[8] respectively (Figure 1).

Examination of published views of a close analog of BILN-2061 bound to the 1−180 protease domain of NS3 protease[9] suggests that the P2 thiazolylquinoline portion of the inhibitor lies on a relatively featureless enzyme surface with binding interactions that provide little apparent basis for the dramatic potency derived from that moiety (>30 000-fold) in a related series of tripeptide inhibitors.[10] In an effort to rationalize this, we chose to model **1** bound to the full length NS3/4A protein including the significantly larger helicase domain (Figure 2) to determine the extent of any role the helicase could play in inhibitor binding. No full length structures with inhibitors bound are currently available; consequently a published apoenzyme structure[11] was used as the starting point. To mimic the conformational change required to permit inhibitor binding, the six C-terminal residues (DLEVVT) of the helicase domain which lie in the active site of the apo X-ray structure were truncated.

Analysis of **1** docked in the latter structure indicated that the helicase domain can provide a surface over the P2 moiety including a pocket to accommodate the thiazolyl substituent. Specific inhibitor-helicase interactions include His528-carbamate oxygen and Gln526-quinoline. Also apparent from this study is that there is space to accommodate a connection between the carbamate cyclopentane and the quinoline ring. Re-examination of the helicase C-terminus from the apo structure (Figure 3), overlaid with BILN-2061, demonstrates that the side chain of Glu628 occupies the same space as the proposed linker. Together, these observations suggested that an alternative P4 cyclopentyl−P2 quinoline macrocyclization to form a structurally distinct series of inhibitors was feasible.

Initially targeted were carbamate derivatives **3a**−**d** (**3c** docked in Figure 4), in which the P1−P3 macrocyclic linker was disconnected, the proposed P2−P4 linker was formed, and a 3-phenylquinoline P2 was used to facilitate rapid synthesis of a range of analogs. Modeling scores for the different linker lengths by two methods (Table 1) predicted that the 5- and 6-carbon linkers would show the greatest activity.

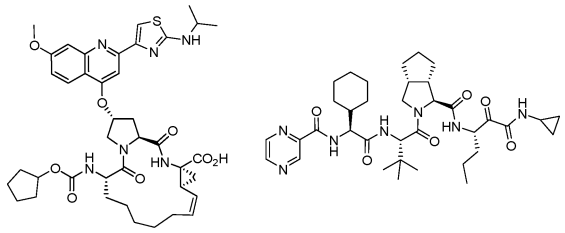

BILN-2061 (**1**) VX-950 (**2**)

Figure 1. NS3/4A protease inhibitors.

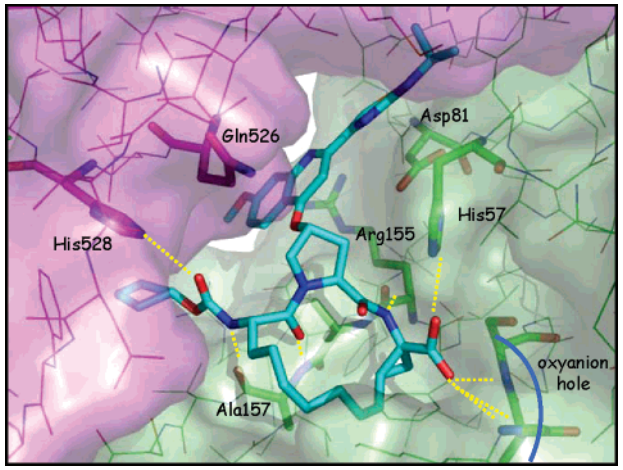

Figure 2. Model of **1** (cyan) bound to full length NS3/4A (protease, green; helicase, purple) with key protein-inhibitor interactions shown.

The desired compounds were prepared as outlined in Scheme 1 via a high yielding ring closing metathesis (RCM) strategy. Displacement of the brosylate of proline derivative **4** with bromohydroxyquinoline **5** yielded ether **6** which was vinylated via palladium catalyzed reaction with tributylvinyltin to give **7**. Subsequent removal of the Boc protecting group and coupling with the appropriate norleucine carbamate derivatives **8a**−**d** afforded key RCM precursors **9a**−**d**. Ring closure was accomplished in excellent yield (84−93%) with 1,3-bis(2,4,6-trimethylphenyl)-4,5-dihydroimidazol-2-ylidene[2-(isopropoxy)-5-(*N*,*N*-dimethylaminosulfonyl)phenyl]methyleneruthenium(II) dichloride (Zhan 1b catalyst) in 1,2-dichloroethane to give macrocyclic olefins **10a**−**d**. Conversion to final products **3a**−**d** was carried out via hydrogena-

† Department of Antiviral Research.
‡ Department of Medicinal Chemistry.
§ Department of Molecular Systems.
|| Department of Drug Metabolism.

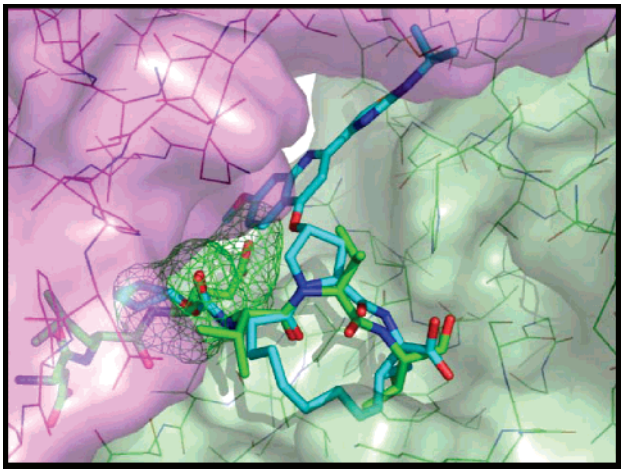

Figure 3. Model of **1** bound to full length NS3/4A with helicase C-terminus (green) restored and Glu628 highlighted with mesh surface.

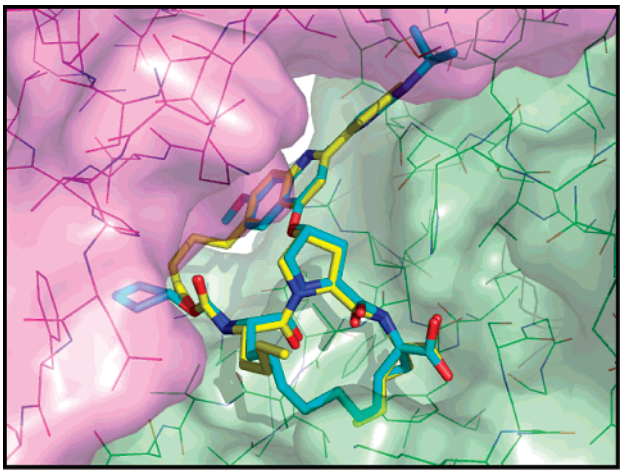

Figure 4. Target macrocycle **3c** (yellow) overlaid with **1.**

Table 1. In Vitro Activity[a]

	modeling			1b replicon IC_{50} (nM)	
compound	E_{inter}[b]	Xscore[b]	1b K_i (nM)	10% FBS	50% NHS
1			0.3	3	19
2			93	1100	4800
3a	−69.5	8.09	2000		
3b	−70.5	8.26	145	6100	>100 000
3c	−71.1	8.36	8.5	1150	5600
3d	−71.4	8.44	25	1200	9100
13			4400		
14			40	4800	>100 000
15			<0.016	6.7	26
16			<0.016	13	25
25a			0.07	4.5	14
25b			0.18	8.7	46

[a] Data are geometric averages of ≥3 determinations. [b] Molecular modeling details in the Supporting Information.

tion of the styryl olefin, hydrolysis of the proline ester, coupling with cyclopropylaminoester **11**[12] to afford **12a**−**d**, and hydrolysis of the P1 ethyl ester.

While **3a**, with the three carbon linker, proved to have very modest activity of 2000 nM in a genotype 1b NS3/4A enzyme inhibition assay[13] (Table 1), incremental lengthening of the linker afforded dramatic improvements with optimized activity of 8.5 nM in the case of the pentyl linker **3c**. A corresponding improvement in genotype 1b cell based replicon activity[14] was also observed. The point of attachment on the quinoline was shown to be critical

Scheme 1. Synthesis of Initial Targets **3a**−**d**[a]

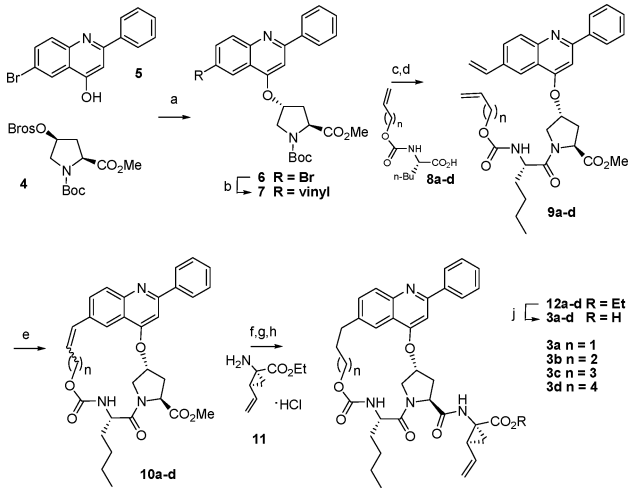

[a] Conditions: (a) Cs_2CO_3, NMP, 40 °C, 86%; (b) $Bu_3SnCH{=}CH_2$, $Pd(PPh_3)_4$, toluene, 100 °C, 79%; (c) 4 N HCl, dioxane; (d) HATU, DIPEA, DMAP, DMF, **8a**−**d**; (e) Zhan 1b catalyst, DCE, ∼10 mM, 84−93%; (f) H_2, 10% Pd/C, EtOAc; (g) LiOH, THF, MeOH, H_2O; (h) HATU, DIPEA, DMAP, **11**, DMF; (j) LiOH, THF, MeOH, H_2O.

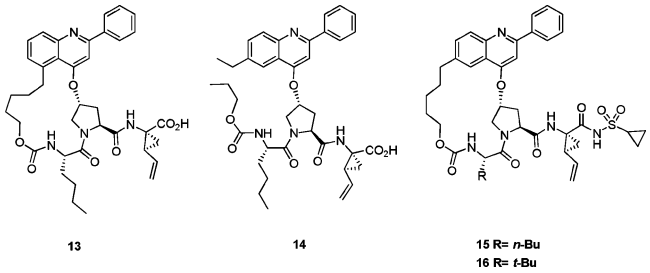

Figure 5. Additional phenylquinoline analogs.

Table 2. Pharmacokinetic Profiles of Key Compounds[a]

compound	C_{max} (nM)	plasma AUC 0-4 h (μM*h)	4 h liver concn (μM)
15	7	<0.01	0.2
16	6	0.01	3.9
25a	240	0.36	18.6
25b	110	0.27	13.4

[a] Compounds dosed at 5 mg/kg P.O. in PEG400 (n = 2−3).

through synthesis of the corresponding 5-substituted derivative **13** by an analogous synthetic route, which proved dramatically less active (K_i 4400 nM). In addition, synthesis of an acyclic analog **14** demonstrated that potency enhancement, particularly in the replicon assay, could be achieved through macrocyclization.

Previous work has established that the carboxylic acid functionality can be effectively replaced with a cyclopropylacylsulfonamide,[15] and application of this strategy to **3c** afforded **15**, with subnanomolar inhibition of NS3/4A protease (K_i <0.016 nM). Disappointingly, given the critical need for liver exposure, oral administration of **15** to rat at 5 mpk P.O. provided low (0.2 μM) compound levels in liver at 4 h with barely detectable plasma exposure (Table 2). In contrast, when the P3 *n*-butyl residue was replaced with *tert*-butyl, the resultant inhibitor **16**, with a very similar in vitro activity profile, was effectively partitioned into liver with a tissue concentration at 4 h of 3.9 μM, although plasma levels were unimproved. The dramatic impact of this minor structural change on liver levels strongly suggests that uptake is via an active transporter mediated process. Having successfully demonstrated that this macrocyclization approach could yield potent compounds with

Scheme 2. Synthetic Approach to Isoquinolines **25a** and **25b**[a]

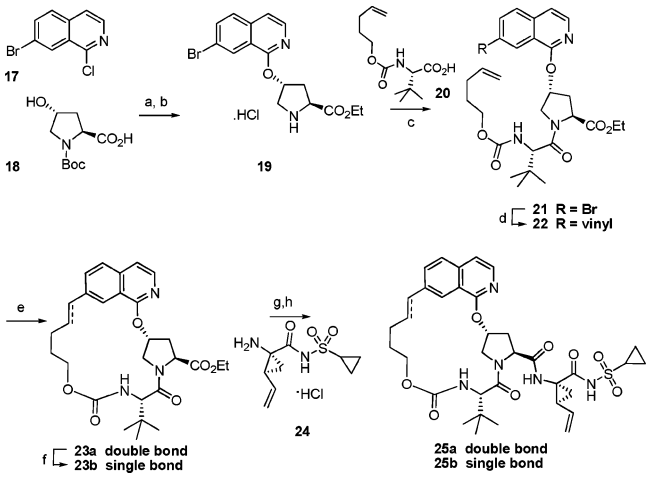

[a] Conditions: (a) KOtBu, DMF; (b) HCl, EtOH, 65% (2 steps); (c) **20**, HATU, DIPEA, DMAP, DMF, 74%; (d) $Bu_3SnCH{=}CH_2$, $Pd(PPh_3)_4$, toluene, 100 °C, 87%; (e) Zhan 1b catalyst, DCE, ~10 mM, 83%; (f) H_2, 10% Pd/C, EtOAc, quant.; (g) LiOH, THF, MeOH, H_2O; (h) HATU, DIPEA, DMAP, **24**, DMF, 93%.

significant liver exposure, we sought to broaden the strategy to include alternative P2 moieties. The use of an isoquinoline P2 to generate potent inhibitors has been reported previously,[16] and an unsubstituted form would also offer somewhat reduced molecular weight inhibitors which might be reflected in improved systemic exposure. To this end, the isoquinoline analogs **25a** and **25b** possessing the optimal five carbon macrocycle linker length were prepared (Scheme 2). Reaction of *trans*-hydroxyproline derivative **18** with 7-bromo-1-chloroisoquinoline **17**, under basic conditions, afforded the crude substitution product which was treated with ethanolic HCl to effect concomitant esterification of the acid and deprotection of the Boc group providing **19** in 65% overall yield. Coupling with the pentenyl carbamate of *tert*-leucine **20** to give **21** (74%) was followed by vinylation to **22** (87%). RCM then afforded almost exclusively *E*-olefin **23a** in 83% isolated yield. Hydrolysis and coupling with aminoacylsulfonamide **24**[16] afforded **25a**. The corresponding saturated analog **25b** was prepared from **23a** analogously, following an initial hydrogenation step. Both analogs showed very potent inhibition in both in vitro enzyme and replicon assays, but, more importantly, liver exposure was dramatically improved with 4 h liver concentrations of 18.6 and 13.4 μM, respectively, for **25a** and **25b**. Furthermore, both compounds were now clearly detectable in plasma with AUCs of 0.36 and 0.27 μM*h, respectively. Sustained exposure in liver is clearly an important factor for any potential treatment for HCV infection, and high compound levels relative to activity in the replicon assay (500 nM, 35 × replicon EC_{50} in the presence of 50% NHS) are maintained in rat liver for 24 h following a 5 mg/kg dose of **25a**.

A detailed evaluation of the more potent analog **25a** revealed no significant activity vs other serine proteases (>50 000-fold selectivity over trypsin and chymotrypsin), hERG binding (IC_{50} >30 μM), or in a broad based Panlabs screen (>4000-fold selectivity). While **25a** has a number of functionalities that might be viewed as potentially susceptible to metabolism, **25a** is primarily excreted in bile as an unchanged parent after rat IV dosing.

An additional attraction of this class of macrocycles is the potential to use a range of macrocyclization strategies in any advanced development including intramolecular Heck or Suzuki reactions, proline amide coupling, or RCM, in contrast to P1−P3 compounds such as **1**, where an RCM step appears unavoidable.[17]

While there are reports of compounds employing a related P2−P4 cyclization strategy,[18,19] the inhibitors had modest micromolar potencies. Synthesis of the cyclopropylacylsulfonamide analog of one of these compounds had little effect on potency.[20]

In summary, molecular modeling of inhibitor bound full length NS3/4A protease structures proved a valuable tool in the design of a new series of potent NS3 protease inhibitors **3a**−**d** which was optimized to compound **25a**. Compound **25a** is accessible via a 9-step longest linear sequence in 35% overall yield leading to a straightforward preparation of >10 g of material. The in vitro activity and selectivity as well as the rat pharmacokinetic profile of **25a** compare favorably with the data for other NS3/4A protease inhibitors currently in clinical development for treatment of HCV infection.

Supporting Information Available: Synthetic procedures and characterization data for new compounds, molecular modeling methods, and complete references for 7a, 7b, 8a, and 14. This information is available free of charge via the Internet at http://pubs.acs.org.

References

(1) WHO. *Weekly Epidemiol. Rec.* **1999**, *74*, 425−427.
(2) Liang, T. J.; Heller, T. *Gastroenterology* **2004**, *127*, S62−S71.
(3) Salmon-Ceron, D.; Lewden, C.; Morlat, P.; Bévilacqua, S.; Jougla, E.; Bonnet, F.; Héripret, L.; Costagliola, D.; May, T.; Chêne, G. *J. Hepatology* **2005**, *42*, 799−805.
(4) Brown, R. S. *Nature* **2005**, *436*, 973−978.
(5) Gordon, C. P.; Keller, P. A. *J. Med. Chem.* **2005**, *48*, 1−20.
(6) For recent reviews, see: (a) Thomson, J. A.; Perni, R. B. *Curr. Opin. Drug Discovery Dev.* **2006**, *9*, 606−617. (b) Chen, S.-H.; Tan, S.-L. *Curr. Med. Chem.* **2005**, *12*, 2317−2342.
(7) (a) Llinas-Brunet, M. et al. *J. Med. Chem.* **2004**, *47*, 1605−1608. (b) Lamarre, D. et al. *Nature* **2003**, *426*, 186−189.
(8) (a) Perni, R. B. et al. *Antimicrob. Agents Chemother.* **2006**, *50*, 899−909. (b) Lin, C.; Kwong, A. D.; Perni, R. B. *Infect. Disord.: Drug Targets* **2006**, *6*, 3−16.
(9) Tsantrizos, Y. S.; Bolger, G.; Bonneau, P.; Cameron, D. R.; Goudreau, N.; Kukolj, G.; LaPlante, S. R.; Llinas-Brunet, Nar, H.; Lamarre, D. *Angew. Chem., Int. Ed.* **2003**, 42, 1356−1360.
(10) LaPlante, S. R.; Llinas-Brunet, M. *Curr. Med. Chem.- Anti-Infective Agents* **2005**, *4*, 111−132.
(11) Yao, N.; Reichert, P.; Taremi, S. S.; Prosise, W. W.; Weber, P. C. *Structure* **1999**, *7*, 1353−1363.
(12) Beaulieu, P. L.; Gillard, J.; Bailey, M. D.; Boucher, C.; Duceppe, J.-S.; Simoneau, B.; Wang, X.-J.; Zhang, L.; Grozinger, K.; Houpis, I.; Farina, V.; Heimroth, H.; Krueger, T.; Schnaubelt, J. *J. Org. Chem.* **2005**, *70*, 5869−5879.
(13) Mao, S.-S.; DiMuzio, J.; McHale, C.; Burlein, C.; Olsen, D. B.; Carroll, S. S. *Anal. Biochem.* **2008**, *373*, 1−8.
(14) Migliaccio, G. et al. *J. Biol. Chem.* **2003**, *278*, 49164−49170.
(15) Tu, Y.; Scola, P. M.; Good, A. C.; Cambell, J. A. *WO2005/054430*, **2005**.
(16) Wang, X. A.; Sun, L.-Q.; Sit, S.-Y.; Sin, Y.; Scola, P. M.; Hewawasam, P.; Good, A. C.; Chen, Y.; Campbell, J. A. *US 6,995,174*, **2006**.
(17) Nicola, T.; Brenner, M.; Donsbach, K.; Kreye, P. *Org. Process Res. Dev.* **2005**, *9*, 513−515.
(18) Marchetti, A.; Ontoria, J. M.; Matassa, V. G. *Synlett* **1999**, *S1*, 1000−1002.
(19) Chen, K. X.; Njoroge, F. G.; Pichardo, J.; Prongay, A.; Butkiewicz, N.; Yao, N.; Madison, V.; Girijavallabhan, V. *J. Med. Chem.* **2006**, *49*, 567−574.
(20) Incorporation of the cyclopropylacyclsulfonamide into **26**[19] (K_i 2100 nM) afforded **27** (K_i 300 nM).

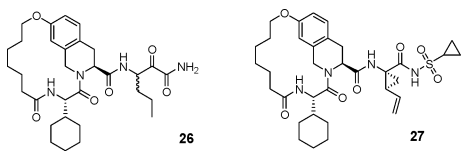

JA711120R